PCCP

Sulfur Kβ X-ray Emission Spectroscopy: Comparison with Sulfur K-edge X-ray Absorption Spectroscopy for Speciation of Organosulfur Compounds

Journal:	*Physical Chemistry Chemical Physics*
Manuscript ID	CP-ART-10-2020-005323.R1
Article Type:	Paper
Date Submitted by the Author:	26-Nov-2020
Complete List of Authors:	Qureshi, Muhammad; Stanford Synchrotron Radiation Lightsource Nowak, Stanislaw; Stanford Synchrotron Radiation Lightsource Vogt, Linda; University of Saskatchewan, Department of Geological Sciences Cotelesage, Julien; University of Saskatchewan, Geological Sciences Dolgova, Natalia; University of Saskatchewan, Geological Sciences Sharifi, Samin; Chevron Energy Technology Company Kroll, Thomas; SLAC National Accelerator Laboratory, SSRL Nordlund, Dennis; Stanford Synchrotron Radiation Lightsource, Mori, Roberto; SLAC National Accelerator Laboratory Weng, Tsu-Chien; Stanford Synchrotron Radiation Lightsource Pickering, Ingrid; University of Saskatchewan, Geological Sciences George, Graham; University of Saskatchewan, Department of Geological Sciences Sokaras, Dimosthenis; SLAC National Accelerator Laboratory, Stanford Synchrotron Radiation Lightsource

Sulfur Kβ X-ray Emission Spectroscopy: Comparison with Sulfur K-edge X-ray Absorption Spectroscopy for Speciation of Organosulfur Compounds

Muhammad Qureshi,[†] Stanisław H. Nowak,[†] Linda I. Vogt,[‡] Julien J. H. Cotelesage,[‡] Natalia V. Dolgova,[‡] Samin Sharifi,[×] Thomas Kroll,[†] Dennis Nordlund,[†] Roberto Alonso-Mori,[Δ] Tsu-Chien Weng,[†,ǁ] Ingrid J. Pickering,[‡,¶] Graham N. George,*[,‡,¶] Dimosthenis Sokaras *[,†]

[†] Stanford Synchrotron Radiation Lightsource, SLAC National Accelerator Laboratory, Stanford University, Menlo Park, California 94025, USA

[‡] Molecular and Environmental Sciences Group, Department of Geological Sciences, University of Saskatchewan, Saskatoon, Saskatchewan S7N 5E2, Canada

[×] Chevron Energy Technology Company, Richmond, California 94802 USA

[Δ] Linear Coherent Light Source, SLAC National Accelerator Laboratory, Stanford University, Menlo Park, California 94025, USA

[ǁ] School of Physical Science and Technology, ShanghaiTech University, Shanghai 201210, China

[¶] Department of Chemistry, University of Saskatchewan, Saskatoon, Saskatchewan S7N 5C9, Canada

ORCID:
Muhammad Qureshi: orcid.org/0000-0001-5700-115X
Stanisław H. Nowak: orcid.org/0000-0002-1575-8370
Linda I. Vogt: orcid.org/0000-0002-0835-0457
Natalia V. Dolgova: orcid.org/0000-0002-9951-6634
Samin Sharifi: orcid.org/0000-0002-9390-3035
Thomas Kroll: https://orcid.org/0000-0003-2176-6905
Dennis Nordlund: https://orcid.org/0000-0001-9524-6908
Ingrid J. Pickering: orcid.org/0000-0002-0936-2994
Graham N. George: orcid.org/0000-0002-0420-7493
Dimosthenis Sokaras: orcid.org/0000-0001-8117-1933

Abstract

Until recently, sulfur was known as a "spectroscopically silent" element because of a paucity of convenient spectroscopic probes suitable for *in situ* chemical speciation. In recent years the technique of sulfur K-edge X-ray absorption spectroscopy (XAS) has been used extensively in sulfur speciation in a variety of different fields. With an initial focus on reduced forms of organic sulfur, we have explored a complementary X-ray based spectroscopy – sulfur Kβ X-ray emission spectroscopy (XES) – as a potential analytical tool for sulfur speciation in complex samples. We compare and contrast the sensitivity of sulfur Kβ XES with that of sulfur K-edge XAS, and find differing sensitivities for the two techniques. In some cases an approach involving both sulfur K-edge XAS and sulfur Kβ XES may be a powerful combination for deducing sulfur speciation in samples containing complex mixtures.

1 Introduction

The organic compounds of sulfur are abundant in nature. Sulfur is amongst the six major elements of life – namely carbon, hydrogen, nitrogen, oxygen, phosphorus and sulfur – which comprise the vast majority of biological molecules. Sulfur compounds are a major component of fossil fuels,[1] the removal of which provides challenges to the fuel industry. Sulfur compounds also show profound involvement in environmental chemistry, and are thought to be important in modulating the effects of climate change.[2,3] Further afield, sulfur is the tenth most abundant element in the universe, with organo-sulfur compounds having been detected in star-forming regions of interstellar space;[4] a variety of organo-sulfur compounds, including thiophenes, thiols and sulfides, also have recently been detected in 3-billion-year-old Martian mudstones by NASA's Curiosity rover.[5]

Sulfur has also been called a "spectroscopically silent" element[6] because until recently there were no convenient spectroscopic probes suitable for *in situ* chemical speciation. Thus, in contrast to phosphorus, its neighbor in the periodic table, sulfur lacks a convenient NMR probe; ^{33}S-NMR is of limited use due to low natural abundance, a small nuclear magnetic moment and large nuclear electric quadrupole couplings.[7] Sulfur K-edge X-ray absorption spectroscopy (XAS), which has been discussed as a possible solution to this deficiency,[6,8] is now acknowledged as a powerful tool,[9–14] that has found applications in fields ranging from geochemistry[15] and fuel science[16–23] to environmental chemistry[24–26] and archaeology,[27] to biological chemistry.[8,28–37] XAS is dominated by intense dipole-allowed $\Delta l=\pm 1$ transitions, which probe the unoccupied molecular orbitals of a system. The technique effectively gives local sulfur-specific speciation information, essentially determining sulfur functional groups; XAS typically cannot identify specific molecular entities, so that (for example) the aliphatic sulfides

methionine and dimethylsulfide are not distinguishable by XAS,[8,12] whereas the thiol cysteine can be distinguished from the sulfide methionine.[8] In complex mixtures this site-selective sensitivity is a distinct advantage, as analysis using a method that was sensitive to individual molecular entities would quickly become intractable. For example, methionine in biological systems will be present in a vast number of different specific molecular entities including many proteins, but sulfur speciation in terms of methionine, as the only organic sulfide that is expected to be present, allows an analysis of the sulfur-specific metabolome.[8]

In comparison to XAS, sulfur Kβ X-ray emission spectroscopy (XES) has been explored relatively little,[38–43] although applications of this method predate those of XAS.[44] Intense XES features are also dipole-allowed $\Delta l=\pm 1$ transitions, albeit from occupied molecular orbitals to fill the 1s core hole created by the primary photoexcitation event. Experimentally, XES typically uses incident exciting X-ray energies that are far from an absorption edge and would more accurately be called non-resonant XES (NR-XES). For sulfur, both the Kα and Kβ XES are accessible, originating from 2p→1s and 3p→1s transitions, respectively. The Kα region is comprised of the Kα1, Kα2 doublet which respectively arises from $2p_{3/2}\rightarrow 1s$ and $2p_{1/2}\rightarrow 1s$ transitions, plus the Kα', Kα3 and Kα4 satellite peaks, which are due to 2p→1s transitions occurring in the presence of spectator 2p holes. Previous work has shown that the Kα12 region exhibits clear chemical shifts, which are slightly greater for the satellites lines,[39,45] but with little change in the structure, which is expected as the transitions are relatively deep-atomic. Notwithstanding this limitation, Kα XES has been used to provide chemical speciation information.[46] Figure 1 compares the sulfur Kα and Kβ XES with the K-edge XAS spectra for two simple species; an aqueous solution of sulfate and a xylene solution of the α-allotrope of elemental sulfur. The ~1.35 eV chemical shift of the Kα doublet between elemental sulfur and

sulfate is clearly seen. As might be expected, the Kβ XES shows considerably greater chemical sensitivity[39] in terms of fine structure compared with the Kα XES (e.g. Figure 1), which is due to the greater involvement of the 3p manifold in chemical bonding. Kβ XES shows promise as either a parallel or an alternative tool to XAS, sharing many of the strengths of the method but with the substantial advantage that measurements can in principle be made using laboratory X-ray sources, whereas for XAS the energy tunability of synchrotron radiation is normally needed. Thus, like XAS, XES can be applied to the study of elements in almost any sample, including those containing complex mixtures of species.

Here we report upon the sulfur Kβ XES of selected organic compounds of sulfur, comparing and contrasting its sensitivities with that of sulfur K-edge XAS. We compare the potential of the two techniques to quantify sulfur chemical forms in a complex mixture, both alone and in combination, using least-squares fitting of spectra. We also show density functional theory (DFT) calculations of the ground state can be used to accurately represent the XES, and to develop an understanding of the factors governing their variability.

2 Experimental

Chemicals and reagents

Reagents and solvents were purchased from Sigma-Aldrich Chemical Company (St. Louis MI, USA), and reagents were of the highest quality available.

X-ray absorption and emission spectroscopy

Sulfur K-edge X-ray absorption spectra (XAS) were recorded on solutions with concentrations of 100 mM. Solutions were placed in SPEX CertiPrep (Metuchen NJ, USA) X-cell sample cups

employing a 3 μm thick Etnom® window (Chemplex Industries, Inc, Palm City FL, USA) to transmit the X-ray fluorescence. Sulfur K-edge XAS was measured at the Stanford Synchrotron Radiation Lightsource (SSRL) on beamline 4-3 using a Si(111) double crystal monochromator, with the cutoff energy of the upstream bare silicon mirror set below 6 keV to reject harmonics. In order to minimize atmospheric attenuation of the X-rays, the experiment was maintained in an atmosphere of helium gas.

Sulfur Kβ non-resonant X-ray emission spectra (XES) were recorded on SSRL beamline 6-2 using a Si(111) double crystal monochromator. X-ray emission spectra were collected using a high-energy resolution X-ray spectrometer specifically designed for the tender X-ray regime (1.6–5.0 keV).[47] The spectrometer uses a cylindrically bent Si(111) Johansson-geometry crystal analyzer, with the sample located inside the Rowland circle so that the spectrometer operates in an energy dispersive mode with readout using a position sensitive detector (CCD camera). The spectrometer energy resolution at the vicinity of the sulfur Kβ emission range is about 0.32 eV.[47] The design of the spectrometer allows the dispersive optics to be maintained under vacuum, with a separate helium-filled chamber enclosing the sample to allow solutions to be measured. An incident X-ray energy of 2850 eV was used for all XES measurements reported here.

Samples for XES were either contained in static liquid sample cuvettes identical to those used on SSRL 4-3 for XAS, or alternatively used a specially constructed recirculating liquid jet flow system with a 250μm Kapton capillary, the 250μm diameter jet was found to be stable at flow rates of approximately ~7ml·min^{-1}. All measurements were optimized accordingly to prevent any spectral modifications from the incident radiation damage.

The incident X-ray energy was calibrated with reference to the lowest-energy sulfur K-edge peak in the XAS spectrum of a sodium thiosulfate standard, which was assumed to be 2469.2

eV.[48] For all samples, the XES energy scale was calibrated with high accuracy by moving the incident X-ray energy to 2470 eV, which is within the range of the XES spectrometer, and employing the elastic scatter peak of the incident X-ray beam as the reference energy.

Analysis of sulfur K-edge XAS data used the EXAFSPAK program suite.[49] Data were normalized to the edge-jump to give a per-unit-sulfur absorption spectrum using the spline method, which employs a rigid spline above the absorption edge to estimate the edge jump. Sulfur Kβ XES spectra were extracted using the analysis procedure described by S. Nowak et al.[47] The spectra were normalized using the integrated area of the Kβ XES.

Density functional theory calculations

All geometry optimizations and first-principle XES calculations were performed using the DFT code ORCA (version 4.2).[50] Computations were performed using the UKS B3LYP functional with the DKH2 relativistic approximation and the CPCM solvation model.[51] All calculated XES spectra were shifted 46.6 eV to align computed and experimental data. Simulated spectra were calculated from the shifted ORCA stick transitions spectra using a custom peak convolution program OFIT.

3 Results and discussion

Experimental accessibility and concentration limits

The utility of sulfur K-edge XAS as a practical tool for speciation is strongly linked to its concentration sensitivity. For biological tissues, typical total sulfur levels are usually equivalent to a concentration of approximately 100 mM,[8,35,36] and for fossil fuels the levels of sulfur vary between 0.1 and 8 wt.%, which corresponds to effective concentration range of approximately 30

mM–2.5 M, with most samples containing around 0.3 wt.% (~100 mM) . With XAS, spectra from samples having high sulfur concentrations are distorted by fluorescent self-absorption phenomena,[28,29] which means that samples must often be diluted to concentrations below about 100 mM in sulfur in order to obtain undistorted spectra. With XES, because the energies of emissions lie below the absorption edge, and because the change in X-ray attenuation coefficient is small across the range of XES spectra, no self-absorption distortions of the spectra are anticipated, although overall intensities will not be linearly proportional to sulfur levels for high concentration samples. In preliminary experiments we examined sulfur Kβ XES spectra for a series of different concentrations; selected results are shown in Figure 2. We find that, using the spectrometer that is currently available to us,[47] sulfur Kβ XES data with acceptable signal to noise can readily be collected within few minutes even for concentrations down to 100 mM, and that as expected no distortion of the spectra is observed at high concentrations.

This establishes the potential of sulfur Kβ XES as a practical tool for sulfur speciation of a range of samples, including biological tissues and fossil fuels. We now proceed to examine the speciation sensitivity of sulfur Kβ XES relative to the better-established sulfur K-edge XAS. The sulfur Kβ XES and sulfur K-edge XAS of a range organosulfur compounds are compared in Figures 3–5.

Comparing XES and XAS of disulfide, sulfide and thiol

Figure 3 compares three aliphatic organo-sulfur compounds: a disulfide (R–S–S–R), a sulfide (R–S–R) and a thiol (R–SH). As we have reported previously,[8] the XAS spectra differ quite significantly between the three categories of compound. The XAS of disulfides is characterized by two intense and clearly resolved features in the spectrum, at around 2469.8 and 2471.3 eV,

attributable to transitions of the sulfur 1s electron to (S–S)σ* and (S–C)σ* unoccupied molecular orbitals[14] which correspond to the lowest unoccupied molecular orbital (LUMO) and the LUMO+1, respectively.[14] Comparing chemical sensitivity of disulfides R–S–S–R having different R groups, we have found that the energies of the S1s→(S–S)σ* change only subtly, whereas the S1s→(S–C)σ* shifts energy in a near-linear manner with the electron withdrawing or donating capacity of the group R.[14] The XAS of organic sulfides can also be characterized by two intense transitions which are closer in energy, that can be assigned as S1s→(S–C)σ* and S1s→(S–C)π* transitions.[12,13] The XAS of thiols appears quite similar to that of sulfides, and also contain two intense features that are close in energy, which are attributable to S1s→(S–H)/(S–C)σ* and S1s→(S–C)σ* transitions.[52,53] With XAS, the spectral features of thiols are shifted subtly to lower energies relative to those of sulfides, so that for systems with well-defined compositions such as tissues where the primary sulfide is methionine and the primary thiol is cysteine, discriminating thiols and sulfides by XAS is possible.[8]

In contrast to the XAS, the XES spectra appear nearly identical between the three types of compound. All spectra exhibit an intense peak at 2466.2 eV and a broader less intense peak at 2464.2 eV. Because of this similarity, and in contrast to sulfur K-edge XAS, sulfur Kβ XES cannot be used to distinguish between the three categories of compounds – disulfide, thiol and sulfide – illustrated in Figure 3.

Sterically hindered sulfides

Figure 4 shows a comparison of the sulfur Kβ XES and sulfur K-edge XAS of a series of sterically hindered sulfides. Previously we have reported that the XAS changes in a systematic manner for sterically hindered sulfides comprised of 4-, 5- and 6-membered rings.[12] In such

systems the 1s→(S–C)σ* and 1s→(S–C)π* transitions in the XAS, to the LUMO and LUMO+1, respectively, are sensitive to the presence of strain in the C–S–C angle, with the 1s→(S–C)σ* shifting to lower energies with increasing ring strain.

The major feature of the sulfur Kβ XES at 2466.2 eV shows little change in the series of compounds investigated. The XES spectra also show a less intense but more complex structure centred at higher energy around 2463.3 eV; this structure shows increasing complexity with increasing ring strain. With the five-membered ring, two intense features at 2464.0 eV and 2462.8 eV are observed in the XES, with lower intensity features at 2459.2 eV and 2456.0 eV. The spectrum of the most strained four-membered ring system shows more complexity still, with a cluster of at least three peaks at 2464.4 eV, 2463.1 eV and 2462.0 eV in the secondary feature, and smaller transitions at 2459.9 eV and one or more weak features at approximately 2453.9 eV. Thus, while the XES shows some subtle variation between this series of sterically hindered sulfides, the XAS is much more distinctive in discriminating between them.

Thiophenic compounds

Figure 5 shows a comparison of the sulfur Kβ XES and sulfur K-edge XAS of selected thiophenic compounds. Thiophenes differ from the systems discussed so far in that they contain aromatic sulfur, with the chalcogen contributing two electrons to the aromatic sextet. In contrast to sulfides and thiols, biological systems do not commonly contain thiophenic forms, although some plant species, in particular those of the genus *Tagetes* (commonly called marigolds) synthesize a range of thiophenes as biocides.[54] Conversely thiophenes, as highly stable molecules, comprise a significant fraction of the sulfur compounds that are found in fossil fuels.[17] We have previously reported on the XAS of a large number of substituted thiophenes.[9]

The XAS spectra comprised two intense transitions in the near-edge region, a 1s→(S–C)π* transition corresponding to the LUMO and a 1s→(S–C)σ* corresponding to the LUMO+1. As with the disulfides,[14] these assignments were confirmed by polarized single crystal XAS measurements. [9]

The sulfur Kβ XES spectra of Figure 5, while broadly similar to each other, are quite distinct from the XES of sulfur forms discussed so far in Figures 3 and 4. Thus, for the previous sulfur forms the highest energy emission peak is also the most intense, whereas for thiophenes the lower energy structure at about 2464 eV is the most intense, with the highest energy feature, at 2466.5–2467.4 eV, having lower intensity. In the sulfur K-edge XAS of substituted thiophenes, the energies of the 1s→(S–C)π* and 1s→(S–C)σ* transitions show systematic changes with the electron withdrawing or donating capacity of the substituent (e.g. thiophene and thiophene 2-carboxaldehyde in Figure 5). In the case of thiophene 2-carboxaldehyde a distinctive lowering of the 1s→(S–C)π* transition energy relative to that of thiophene is observed, and a more subtle increase in energy of the 1s→(S–C)σ* transitions.[9] Whereas the XAS of thiophene and thiophene 2-carboxaldehyde are quite distinct, the sulfur Kβ XES spectra show only subtle differences.

As we have previously discussed, [9] for many thiophenes the 1s→(S–C)π* and 1s→(S–C)σ* transitions overlap in energy, which results in the observation of a single thiophenic peak in XAS of hydrocarbon fuels and related materials.[17] Thus, benzothiophene and dibenzothiophene exhibit very similar XAS (Figure 5), making these compounds difficult to distinguish by this method, especially in complex mixtures. In contrast to this observation, the sulfur Kβ XES spectra of benzothiophene and dibenzothiophene are quite distinct (Figure 5), with the highest energy

emission shifted to high energy with increased nuclearity. Thus, the increased extent of the ring system is more distinguishable in XES compared with XAS.

Density functional theory calculations

In principle at least, XES spectra are more accessible to computation using quantum mechanical approaches than are XAS spectra. This is because, unlike XAS, the ground state molecular orbital energies provide a good basis for computing the valence to core transitions which comprise the XES. A variety of approaches have been reported in previous work; early studies used semi-empirical MNDO and *ab initio* STO-3g approaches, with some success.[55,56] More recent studies have used density functional theory to model sulfur Kβ XES.,[57] Most recently, the use of linear-response time-dependent density functional theory (LR-TDDFT)[58] has been applied to model a wide variety of sulfur Kβ XES data,[59] with some new experimental data, and with many spectra digitized from the early work of Yasuda and Kakiyama[39] and Alonso-Mori et al.[43] This work showed that the LR-TDDFT approach required smaller shifts between experimental and computed spectra across different sulfur oxidation states than a simpler ground state based approach.[59] Our XES calculations used the ORCA package,[50] and are ground-state based,[60] employing the B3LYP functional with the DKH2 dispersion correction, and triple-ζ valence polarized basis set.

Density functional theory simulations of XES are shown in Figure 6, with all exhibiting a very close correspondence with the experimental XES. Examination of the transition intensities shown in Figure 6 indicates that, while there should be subtle differences between spectra that appear quite similar (e.g. Figure 4), experimental data with substantially improved signal to noise would be needed to distinguish these. Molecular orbitals for selected molecules of Figure 6 are

shown in Figure 7, together with the relevant spectra. In all of the non-aromatic compounds studied the highest occupied molecular orbital (HOMO) is a non-bonding orbital containing a pair of electrons, centred primarily on sulfur, with some (S–C)π* character. The HOMO gives rise to the intense peak in the XES at 2466.2 eV, which has a similar energy for disulfides, thiols and sulfides, as well as changing only subtly as a function of the series of sterically hindered sulfides. Figure 7*a* shows the orbitals for the cyclic organic sulfide, tetrahydrothiophene, which has a small degree of ring strain imposed at the sulfur atom. With simple thiophenes, the HOMO is typically a C=C π-bonding orbital with little sulfur involvement (Figure 7*b*) and therefore contributing little XES intensity. In this case, the HOMO is separated by a fraction of an eV from the HOMO-1 which comprises a lone-pair type orbital with involvement of the having substantial sulfur 3p (47.7%) character (Figure 7*b*); this shows little sensitivity to the presence of ring substituents. Proceeding down in energy, the HOMO-2 through HOMO-5 are both σ and π-bonding orbitals, and are separated from each other by fractions of an eV. These together correspond to the most intense feature in the thiophene XES, and while some of these orbitals are sensitive to the presence of ring substituents the composite effect is one of only subtle sensitivity. In the cases of benzothiophene and dibenzothiophene the more extended polycyclic aromatic system causes a rearrangement of the levels, so that the orbital corresponding to the HOMO-1 in thiophene is now the HOMO, and is shifted to higher energy, which gives the observed shifts of the high-energy peak positions in the XES (Figure 5). A selection of the relevant molecular orbitals of dibenzothiophene is shown in Figure 8. The particular ability of sulfur Kβ XES to distinguish between different thiophenic forms may be of considerable interest in fossil fuel research.

Comparing XAS and XES for quantitative speciation

The use of linear combination analysis for quantitative sulfur K-edge XAS speciation was introduced by Pickering and co-workers.[8] In this method linear combinations of spectra of representative standards are fitted to the spectra of samples of unknown composition with the sum of the squares of differences minimized during the fit. One obvious disadvantage of this method is that standard spectra must be available, and the presence of complete unknowns in a mixture may therefore pose difficulties. To evaluate the relative abilities of XAS and XES in linear combination fitting for speciation of mixtures, we adopted a Monte-Carlo approach by testing synthetic data corresponding to mixtures of selected compounds computed from their measured standard spectra with various levels of added noise incorporated using Poisson distributed statistics. The program used randomly generated fractions of each of five compounds, added Poisson statistical noise, and computed the linear combination analysis using both XAS and XES. The program also randomly eliminated components, so that some mixtures contained fewer than five components. The relative normalization conditions for XAS and XES were carefully adjusted to give equivalent signal to noise conditions. 40 different synthetic mixtures were each subjected to three linear combination analyses for their computed XAS and XES alone, and the combined XAS and XES. The five compounds selected were dibenzothiophene, benzothiophene, aliphatic disulfide (di-*n*-hexyldisulfide), aliphatic sulfide (di-*n*-heptylsulfide) and tetrahydrothiophene. As anticipated from examining the trends in the experimental data in Figures 2-4, the mean difference from the input values was substantially lower for XAS than for XES (Fig. 9), with respective mean differences corresponding to 1.8% and 7.4%. While the sensitivity will obviously strongly depend upon the compounds selected and the level of noise in the synthetic data, nonetheless the fits for this specific set of data contain some interesting trends.

For XAS the spectroscopically most distinct compound is the disulfide, which was much more accurately determined at 0.5% than the other compounds all of which were around 2% (the values were 2.3, 2.0, 0.5, 2.3, 1.9 %, in the order listed above). For XES the best determined compounds were dibenzothiophene at 4.1% and tetrahydrothiophene at 3.9% (the values were 4.1, 5.3, 12.1, 11.4 and 3.9 %, in the order listed above). The worst determined was the disulfide at 12.1% which is expected as this is spectroscopically less distinctive (Fig. 3). These trends were reflected in both the derived values for the estimated standard deviations (Fig. 9) and the covariance values. Finally, the combined linear combination of both XAS and XES showed consistently improved accuracies relative to data from either method with a single exception, with values for the five compounds of 2.2, 1.9, 0.7, 2.1 and 1.6 %, again with the same ordering, and a mean difference of 1.7%. These values are all slightly better than the XAS-alone values, with the exception of that for the disulfide, which gave an error of 0.7% for the combined fit relative to XAS of 0.5%.

XAS has the substantial advantage that it can be collected using fairly standard equipment which is likely to be present on many beamlines, whereas sulfur Kβ XES needs specialized instrumentation, which is currently only available at a handful of facilities.[47] This is particularly true if solutions are to be studied as most infrastructure employ vacuum conditions in the sample chamber. Moreover, at least in our case, sulfur Kβ XES data typically contained somewhat higher noise levels than did the XAS. Conversely, XES can in principle be measured with laboratory-based X-ray sources,[39,59] although dilute solutions might be challenging because of the lower photon fluxes in such instruments, and a specialized high energy resolution detector is needed.

4 Conclusions

Here we have explored the potential of sulfur Kβ XES as an analytical tool for sulfur speciation in complex samples, with a focus on reduced forms of sulfur. We have compared and contrasted the species sensitivity of sulfur Kβ XES with the better-established sulfur K-edge XAS, and find that XAS shows superior sensitivity towards non-aromatic reduced sulfur compounds, while the capabilities of sulfur Kβ XES may be superior for polycyclic aromatic sulfur compounds. We find that sulfur Kβ XES can be adequately modelled from ground state density functional calculations, and that the spectra are readily understood from a simple molecular orbital approach, which may be an advantage over XAS. Tests using linear combination analyses showed that the relative speciation sensitivities of the two methods reflected the spectroscopic distinctiveness of the two methods. A combined approach involving both XES and XAS data may produce better speciation results than either method in isolation, but this will depend strongly upon the compounds involved.

Conflicts of interest

There are no conflicts to declare.

Acknowledgements

Research at the University of Saskatchewan is supported by a grant from the Chevron Energy Technology Company, the Natural Sciences and Engineering Research Council (GNG, IJP), the University of Saskatchewan and by Canada Research Chairs (GNG, IJP). Use of the Stanford Synchrotron Radiation Lightsource (SSRL), SLAC National Accelerator Laboratory, is supported by the U.S. Department of Energy (DOE), Office of Science, Office of Basic Energy Sciences under Contract number DE-AC02-76SF00515, respectively. The SSRL Structural

Molecular Biology Program is supported by the DOE Office of Biological and Environmental Research, and by the National Institutes of Health, National Institute of General Medical Sciences (including P41GM103393). The contents of this publication are solely the responsibility of the authors and do not necessarily represent the official views of NIGMS or NIH. This research used resources of the National Energy Research Scientific Computing Center (NERSC), a U.S. Department of Energy Office of Science User Facility operated under Contract No. DE-AC02-05CH11231.

References

1 A. Demirbas, H. Alidrisi and M. A. Balubaid, *Petrol. Sci. Technol*., 2015, **33**, 93–101.

2 R. J. Charlson, J. E. Lovelock, M. O. Andreae and S. G. Warren, *Nature*, 1987, **326**, 655–661.

3 E. H. Hoffman, A. Tilgner, R. Schrödner, R. Bräuer, R. Wolke and H. Herrmann, *Proc. Natl. Acad. Sci. USA*, 2016, **113**, 11776–11781.

4 L. Kolesniková, B. Tercero, J. Cernicharo, J. L. Alonso, A. M. Daly, B. P. Gordon and S. T. Shipman, *Astrophys. J. Lett.* **2014**, *784*, L7/1–L7/8.

5 J. L Eigenbrode, R. E. Summons, A. Steele, C. Freissinet, M. Millan, R. Navarro-González, B. Sutter, A. C. McAdam, H. B. Franz, D. P. Glavin, P. D. Archer Jr., P. R. Mahaffy, P. G. Conrad, J. A. Hurowitz, J. P. Grotzinger, S. Gupta, D. W. Ming, D. Y. Sumner, C. Szopa, C. Malespin, A. Buch and P. Coll, *Science* 2018, **360**, 1096–1101.

6 F. Jalilehvand, *Chem. Soc. Rev.*, 2006, **35**, 1256–1268

7 L. A. O'Dell and I. L. Mourdrakovski, *J. Magn. Reson.* 2010, **207**, 345–347.

8 I. J. Pickering, R. C. Prince, T. C. Divers and G. N. George, *FEBS Letters*, 1998, **441**, 11–14.

9 G. N. George, M. J. Hackett, M. Sansone, M. L. Gorbaty, S. R. Kelemen, R. C. Prince, H. H. Harris and I. J. Pickering, *J. Phys. Chem. A*. 2014, **118**, 7796–7802.

10 J. J. H. Cotelesage, M. J. Pushie, M. Barney, A. Nissan, I. J. Pickering, L. Vogt and G. N. George *J. Phys. Chem. A*. 2016, **120**, 6929–6933.

11 M. J. Pushie, J. J. H. Cotelesage, L. Vogt, M. Barney, I. J. Pickering and G. N. George, *J. Phys. Chem. A*. 2018, **122**, 3711–3712.

12 J. J. H. Cotelesage, M. Barney, L. Vogt, I. J. Pickering and G. N. George, *J. Phys. Chem. A*., 2017, **121**, 6256–6261.

13 L. I. Vogt, N. V. Dolgova, J. J. H. Cotelesage, M. Barney, S. Sharifi, I. J. Pickering and G. N. George, *J. Phys. Chem. A*. 2019, **123**, 2861−2866.

14 I. J. Pickering, M. Barney, J. J. H. Cotelesage, L. Vogt, M. J. Pushie, A. Nissan, R. C. Prince and G. N. George, *J. Phys. Chem. A*. 2016, **120**, 7279–7286.

15 J. Majzlan, C. N. Alpers, C. B. Koch, R. B. McCleskey, S. C. B. Myneni and J. M. Neil, *Chem. Geol.*, 2011, **284**, 296–305.

16 C. L. Spiro, J. Wong, F. W. Lytle, R. B. Greegor, D. H. Maylotte and S. H. Lamson, *Science*, 1984, **226**, 48–50.

17 G. N. George and M. L. Gorbaty, *J. Am. Chem. Soc*. 1989, **111,** 3182–3186.

18 M. J. Grossman, M. K. Lee, R. C. Prince, K. K. Garrett, G. N. George and I. J. Pickering, *Appl. Environ. Microbiol*. 1999, **65**, 181–188.

19 G. S. Waldo, R. M. K. Carlson, J. M. Moldowan, K. E. Peters and J. E. Penner-Hahn, *Geochim. Cosmochim. Acta* 1991, **55**, 801–814.

20 S. R. Kelemen, C. C. Walters, P. J. Kwiatek, H. Freund, M. Afeworki, M. Sansone, W. A. Lamberti, R. J. Pottorf, H. G. Machel and K. E. Peters, *Geochim. Cosmochim. Acta* 2010, **74**, 5305–5332.

21 A. E. Pomerantz, K. D. Bake, P. R. Craddock, K. W. Kurzenhauser, B. G. Kodalen, S. Mitra-Kirtley and T. B. Bolin, *Org. Geochem*. 2014, **68**, 5-12.

22 G. N. George, M. L. Gorbaty, S. R. Kelemen and M. Sansone, *Energy and Fuels* 1991, **5**, 93–97.

23 F. E. Huggins and G. P. Huffman, *Int. J. Soc. Mater. Eng. Resour*. 2002, **10**, 1–13.

24 M. A. Vairavamurthy, D. Maletic, S. Wang, B. Manowitz, T. Eglinton and T. Lyons, *Energ. Fuel*. 1997, **11**, 546–553.

25 M. J. Morra, S. E. Fendorf and P. D. Brown, *Geochim. Cosmochim. Acta* 1997, **61**, 683–688.

26 J. Majzlan and S. C. B. Myneni, *Environ. Sci. Technol*. 2005, **39**, 188–194.

27 Y. Fors, F. Jalilehvand, R. E. Damian, C. Bjoerdal, E. Phillips and M. Sandström, *J. Archaeol. Sci*. 2012, **39**, 2521–2532.

28 I. J. Pickering, G. N. George, E. Y. Yu, D. C. Brune, C. Tuschak, J. Overmann, J. T. Beatty and R. C. Prince, *Biochemistry* 2001, **40**, 8138–8145.

29 G. N. George, M. Gnida, D. A. Bazylinski, R. C. Prince and I. J. Pickering, *J. Bacteriol*. 2008, **190**, 6376–6383.

30 E. Y. Yu, I. J. Pickering, G. N. George and R. C. Prince, *Biochim. Biophys. Acta* 2001, **1527**, 156–160.

31 I. J. Pickering, C. Wright, B. Bubner, M. W. Persans, E. Y. Yu, G. N. George, R. C. Prince and D. E. Salt, *Plant Physiol*. 2003, **131**, 1460–1467.

32 I. J. Pickering, E. Y. Sneeden, R. C. Prince, H. H. Harris, G. Hirsch and G. N. George, *Biochemistry* 2009, **48**, 6846–6853.

33 E. Y. Sneeden, H. H. Harris, I. J. Pickering, R. C. Prince, S. Johnson, X. Li, E. Block and G. N. George, *J. Am. Chem. Soc*. 2004, **126**, 458–459.

34 P. Frank, B. Hedman and K. O. Hodgson, *J. Inorg. Biochem*. 2014, **131**, 99–108.

35 M. Gnida, E. Y. Sneeden, J. C. Whitin, R. C. Prince, I. J. Pickering, M. Korbas and G. N. George, *Biochemistry*, 2007, **46**, 14735–14741.

36 M. J. Hackett, S. E. Smith, P. G. Paterson, H. Nichol, I. J. Pickering and G. N. George, *ACS Chem. Neurosci*. 2012, **3**, 178–185.

37 M. J. Hackett, G. N. George, I. J. Pickering and B. F. Eames, *Biochemistry*, 2016, **55**, 2441–2451.

38 Y. Takahashi, *Bull. Chem. Soc. Japan*, 1973, **46**, 2039–2044.

39 S. Yasuda and H. Kakiyama, *Spectrochim. Acta*, 1979, **35A**, 485–493.

40 M. Mogi, A. Ota, S. Ebihara, M. Tachibana and M. Uda, *Nucl. Instrum. Methods Phys. Res.*, 1993, **B75**, 20–23.

41 J. Niskanen, C. J. Sahle, K. O. Ruotsalainen, H. Müller, M. Kavčič, M. Žitnik, K. Bučar, M. Petric, M. Hakala and Simo Huotari, *Sci. Rep.* 2016, **6**, 21012/1–8.

42 M. Petric, R. Bohinc, K. Bucar, S. H. Nowak, M. Zitnik and M. Kavcic, *Inorg. Chem.* 2016, **55**, 5328–5336.

43 R. Alonso Mori, E. Paris, G. Giuli, S. G. Eeckhout, M. Kavčič, M. Žitnik, K. Bučar, L. G. M. Pettersson and P. Glatzel, *Inorg. Chem*., 2010, **49**, 6468–6473.

44 Y. Takahshi, K. Yabe and T. Sato, *Bull. Chem. Soc. Japan*, 1969, **42**, 2707–2708.

45 R. Alonso Mori, E. Paris, G. Giuli, S. G. Eeckhout, M. Kavčič, M. Žitnik, K. Bučar, L. G. M. Pettersson and P. Glatzel, *Anal. Chem*., 2009, **81**, 6516–6525.

46 W. M. Holden, G. T. Seidler and S. Cheah, *J. Phys. Chem. A.*, 2018, **122**, 5153–5161.

47 S. H. Nowak, R. Armenta, C. P. Schwartz, A. Gallo, B. Abraham, A. T. Garcia-Esparza, E. Biasin, A. Prado, A. Maciel, D. Zhang, D. Day, S. Christensen, T. Kroll, R. Alonso-Mori, D. Nordlund, T.-C. Weng and D. Sokaras, *Rev. Sci. Instrum.,* 2020, **91**, 033101/1–12.

48 H. Sekiyama, N. Kosugi, H. Kuroda and T. Ohta, *Bull Chem. Soc. Jpn.*, 1986, **59**, 575–579.

49 George, G. N. 2001, http://www-ssrl.slac.stanford.edu/exafspak.html

50 F. Neese, Wiley Interdiscip. Rev.: *Comput. Mol. Sci.*, 2012, **2**, 73–78.

51 D. A. Pantazis, X.-Y. Chen, C. R. Landis and F. Neese, *J. Chem. Theory Comput.*, 2008, **4**, 908–919.

52 C. Dezarnaud, M. Tronc and A. P. Hitchcock, *Chem. Phys*., 1990, **142**, 455–462.

53 S. Beyhan, Y. Hu and S. G. Urquhart, *J. Chem. Phys*. 2011, **134**, 244–304.

54 I. Marotti, M. Marotti, R. Piccaglia, A. Nastri, S. Grandi and G. Dinelli, *J. Sci. Food Agric.*, 2010, **90**, 1210–1217.

55 R. C. C. Perera and R. E. LaVilla, *J. Chem. Phys*., 1984, **81**, 3375–3382.

56 R. C. C. Perera and R. E. LaVilla, *J. Chem. Phys.*, 1986, **84**, 4228–4234.

57 J. Niskanen, C. J. Sahle, K. O. Ruotsalainen, H. Müller, M. Kavčič, M. Žitnik, K. Bučar, M. Petric, M. Hakala and S. Huotari, *Sci. Rep.*, 2016, **6**, 21012/1–7.

58 Y. Zhang, S. Mukamel, M. Khalil and N. Govind, *J. Chem. Theor. Comput.*, 2015, **11**, 5804–5809.

59 W. M. Holden, E. P. Jahrman, N. Govind and G. T. Seidler, *J. Phys. Chem. A*., 2020, **124**, 5415–5434.

60 N. Lee, T. Petrenko, U. Bergmann, F. Neese, S. DeBeer, *J. Am. Chem. Soc.*, 2010, **132**, 9715–9727.

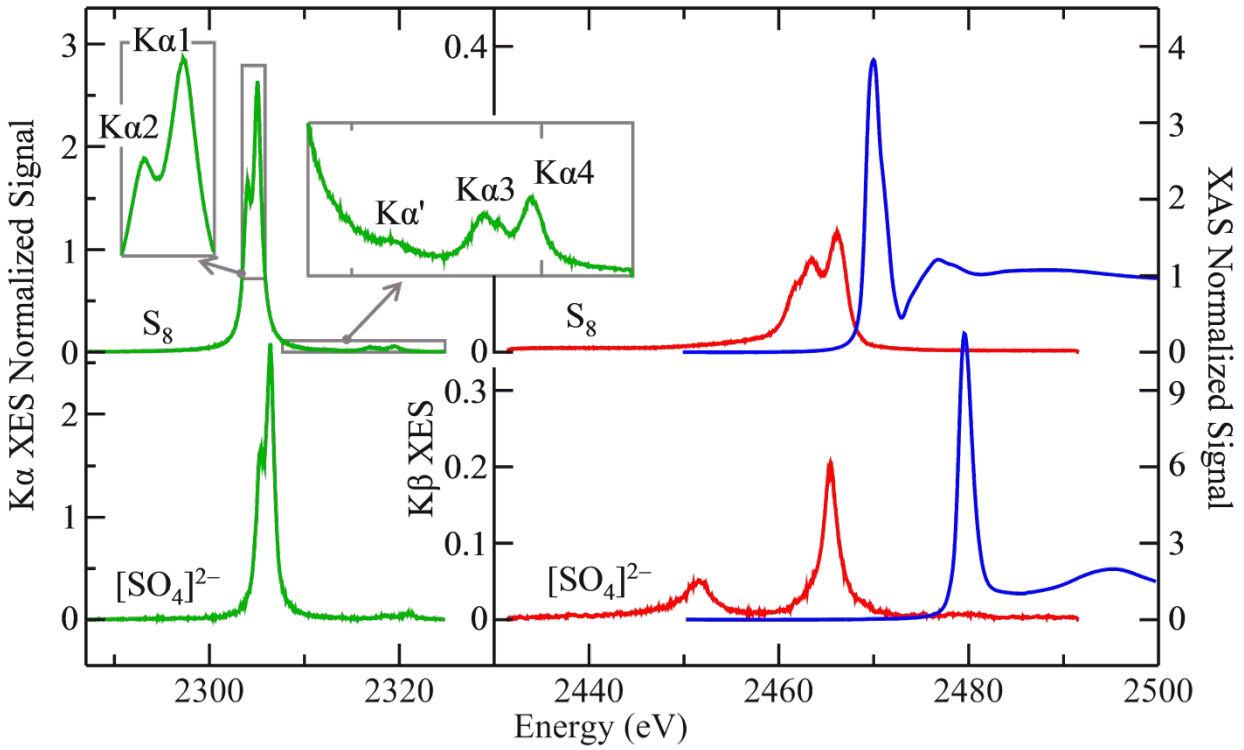

Fig. 1 Comparison of Sulfur XES of 100 mM solutions of elemental α-sulfur (S_8) in xylene and $(NH_4)_2SO_4$ in water at pH 7.4. The figure compares the Kα (green) and Kβ (red) XES with the XAS (blue). The insets (gray boxes) show expanded regions for both the Kα1 Kα2 doublet and the major Kα satellite lines for S_8. The Kα XES show clear chemical shifts, but do not show the substantial spectroscopic differences exhibited by the Kβ XES or the XAS.

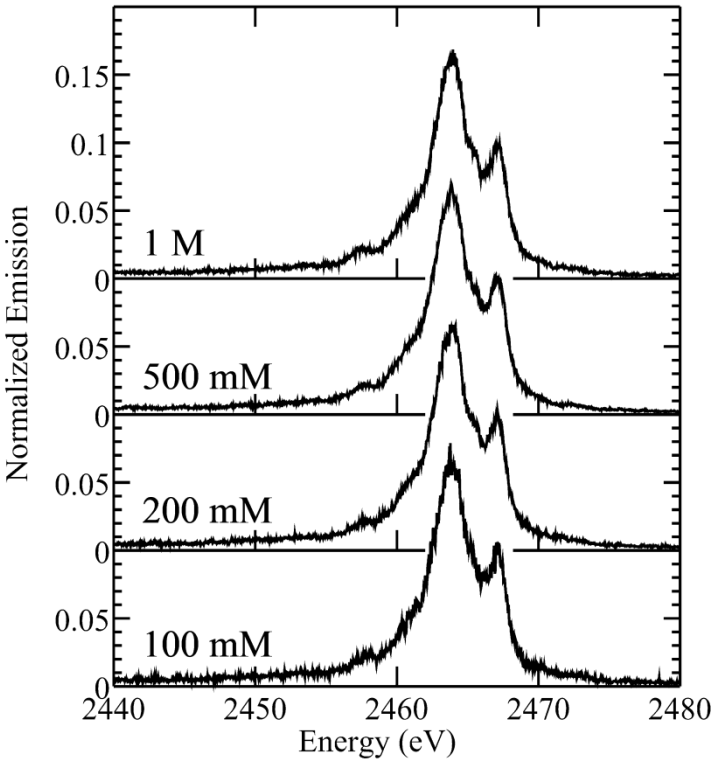

Fig. 2 Sulfur Kβ XES of toluene solutions of benzothiophene standard at different concentrations. Different numbers of sweeps were accumulated to give similar signal to noise ratios for the different concentrations.

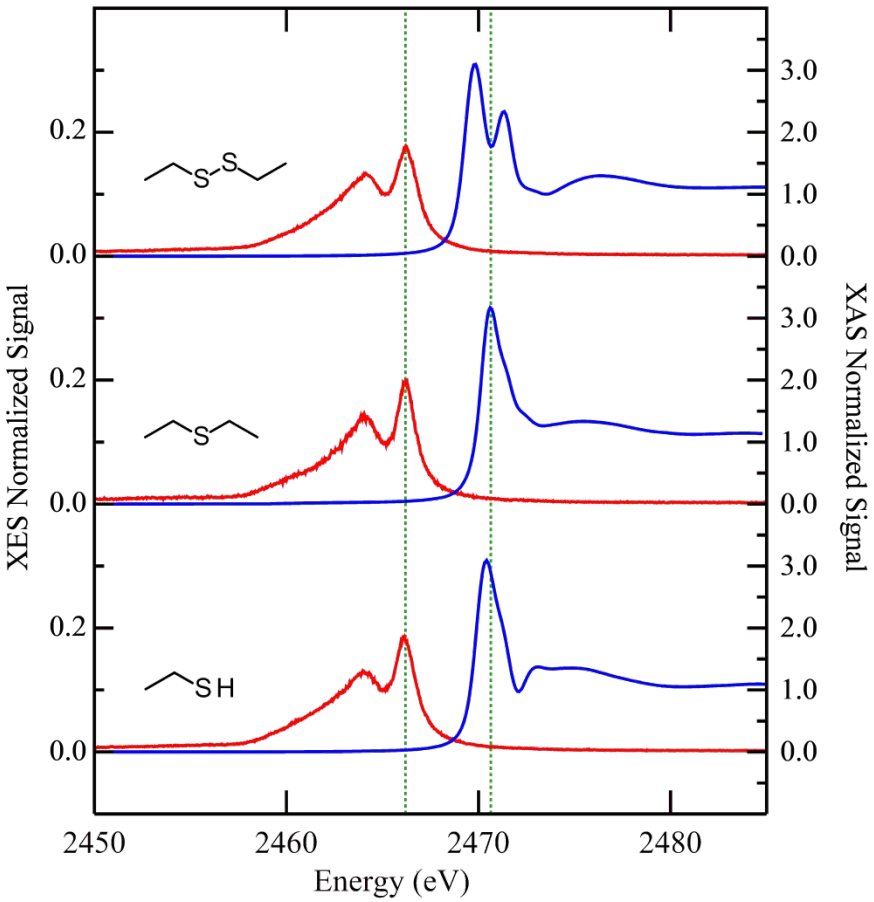

Fig. 3 Sulfur Kβ XES (red lines) and K-edge XAS (blue lines) of an organic aliphatic disulfide (di-*n*-hexyldisulfide), an organic sulfide (di-*n*-heptylsulfide) and a thiol (*n*-heptylthiol). The structures shown adjacent to the spectra are truncated to include the only two carbon atoms nearest to the sulfur. The vertical broken green lines are included to guide the eye to small shifts in the features of the spectra.

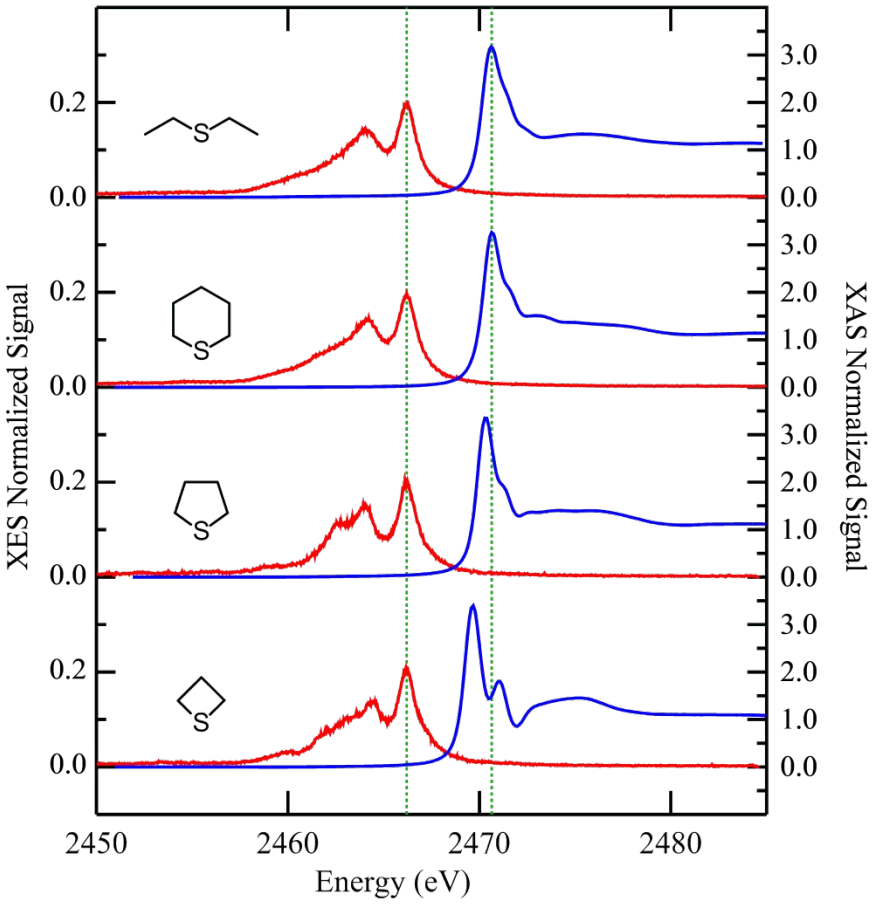

Fig. 4 Sulfur Kβ XES (red lines) and K-edge XAS (blue lines) of sterically hindered and unhindered sulfides. Top to bottom: di-*n*-heptylsulfide (the adjacent structure truncated to include the only two carbon atoms nearest to the sulfur), tetrahydrothiopyran (thiane), tetrahydrothiophene (thiolane), trimethylene sulfide (thietane). The vertical broken green lines (note that these differ in position from those of Figure 3) are included to guide the eye to small shifts in the features of the spectra.

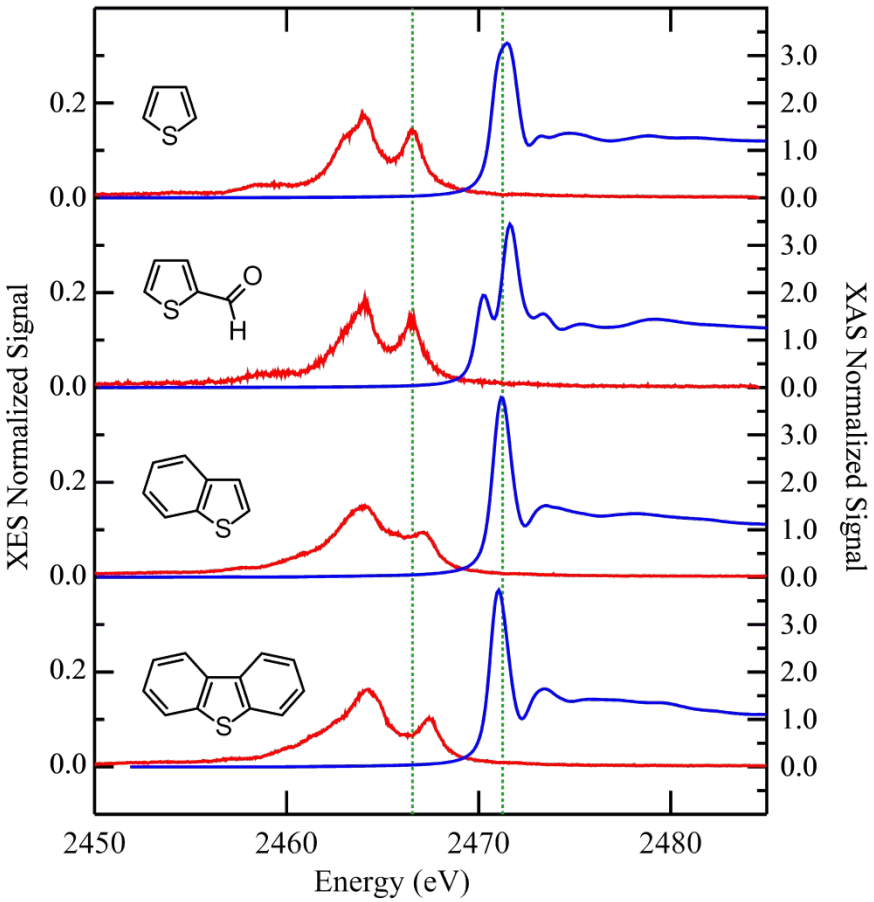

Fig. 5 Sulfur Kβ XES (red lines) and K-edge XAS (blue lines) of thiophenic compounds. Top to bottom: thiophene, thiophene-2-carboxaldehyde, benzothiophene and dibenzothiophene. The vertical broken green lines are included to guide the eye to small shifts in the features of the spectra (note that these differ in position from those of Figures 3 and 4).

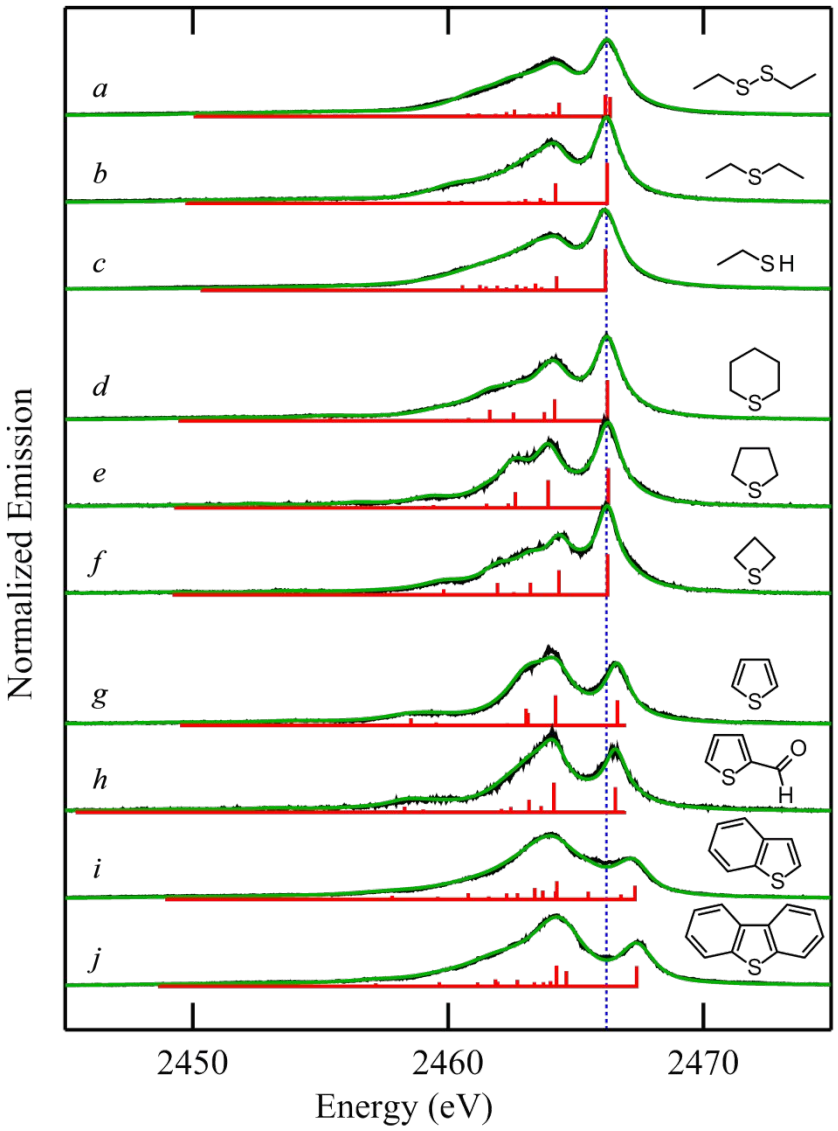

Fig. 6 Results of density functional theory simulations of all the compounds reported in this paper. Experimental data is indicated by the black lines, with the theoretical peak-shape convoluted spectra by the green lines, and the red lines show stick spectra indicating the energies of the computed transitions. Schematic structures for the individual compounds are shown in the insets (right); for *a–c* the schematic structures are truncated to include the two carbon atoms nearest to sulfur. The vertical broken blue line is included to guide the eye to small shifts in the features of the spectra.

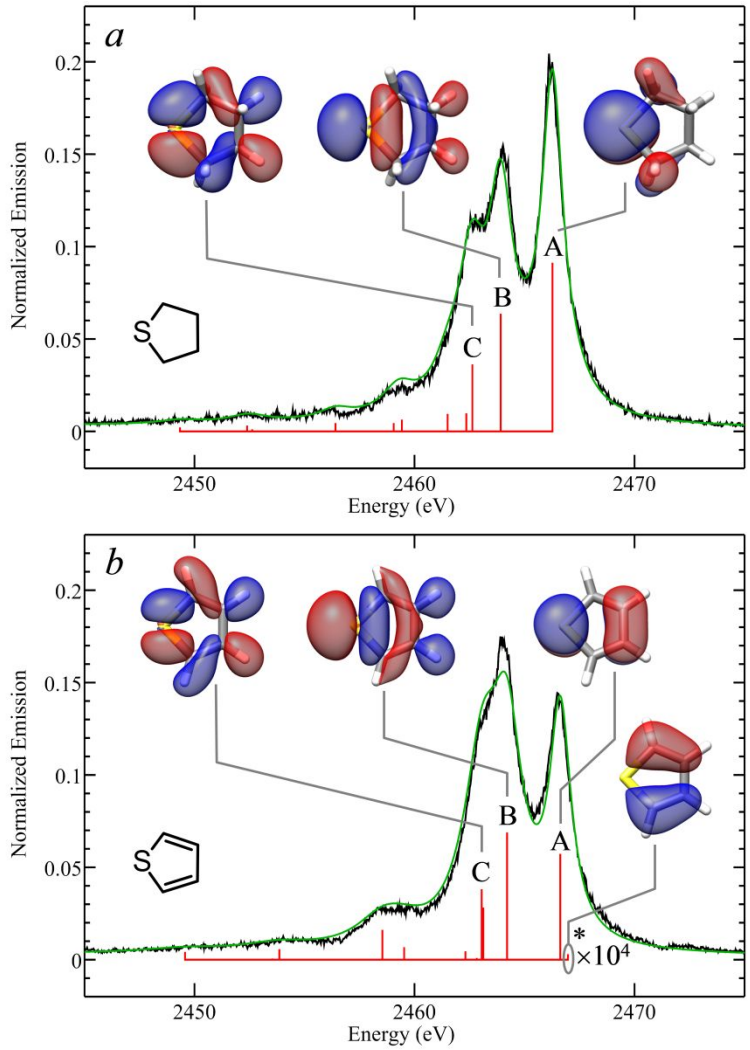

Fig. 7 Molecular orbital isosurfaces for the ground state levels whose decay leads to the sulfur Kβ XES. *a* shows the data for the cyclic aliphatic sulfide tetrahydrothiophene and *b* shows the data for thiophene, the simplest aromatic form. In both cases the black lines show experimental data, green lines the simulated spectra and the red lines show stick spectra indicating the energies of the computed transitions. In *b*, the stick spectrum intensity for the HOMO (marked *) which has very little sulfur involvement, has been increased by 10^4 to show its position.

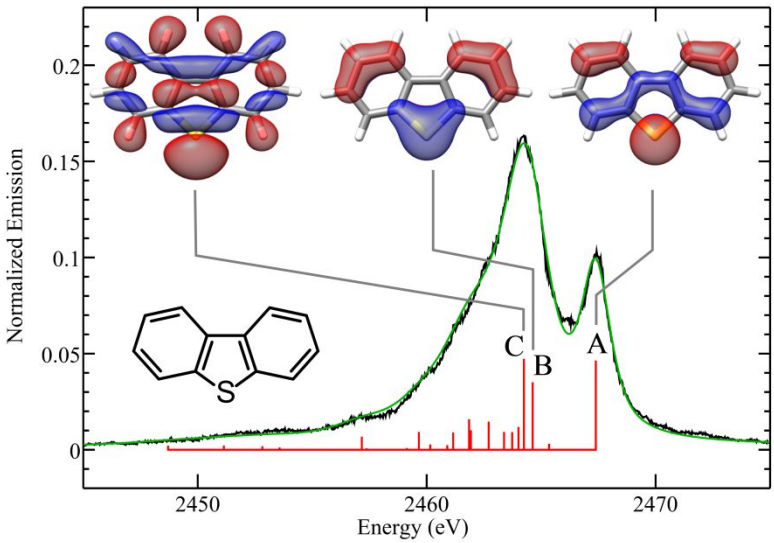

Fig. 8 Molecular orbital isosurfaces for the ground state levels whose decay leads to the sulfur Kβ XES for the polycyclic aromatic sulfur compound dibenzothiophene. The black line shows the experimental data, green line the simulated spectrum and the red lines show the stick spectrum indicating the energies of the computed transitions.

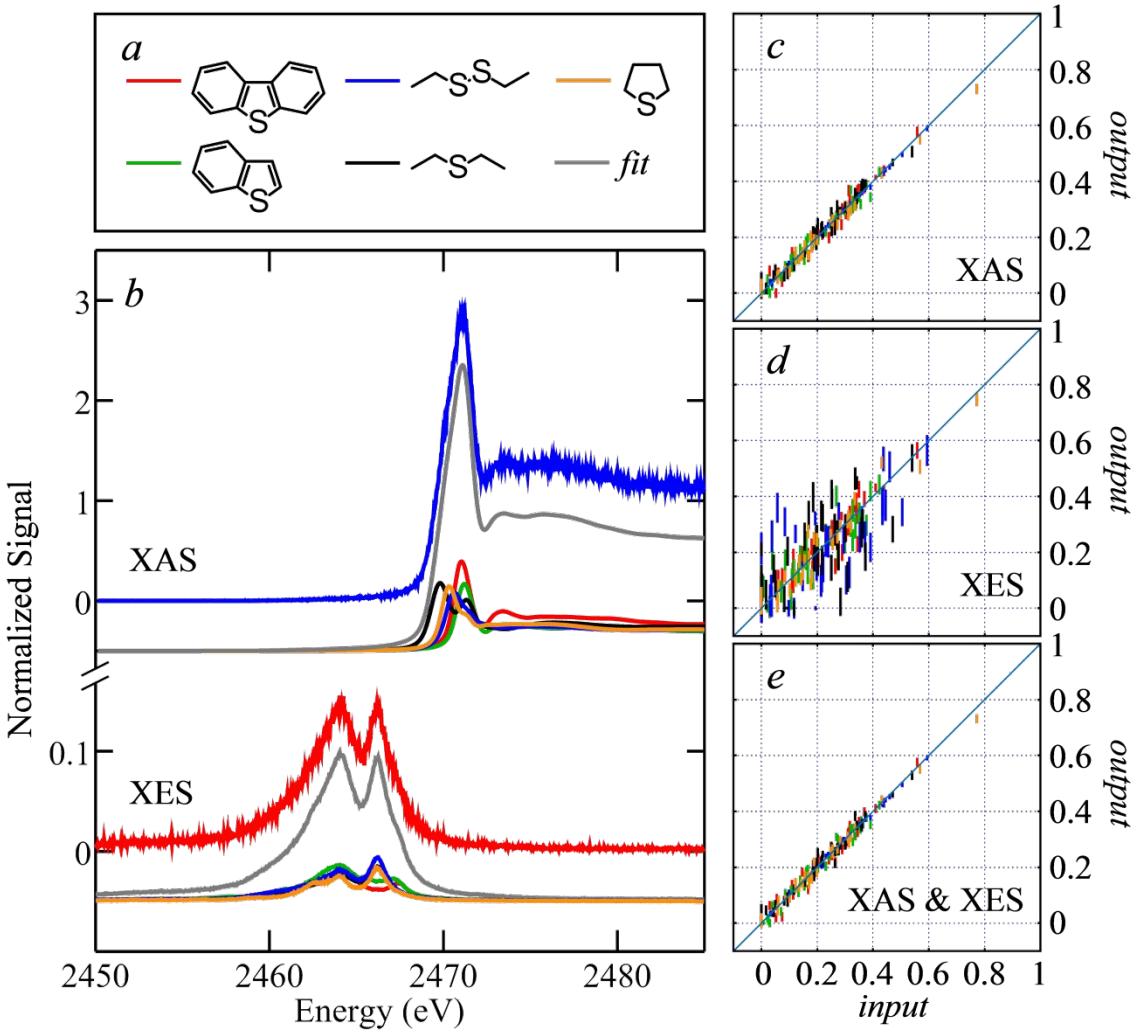

Fig. 9 Linear combination analysis for sulfur K-edge XAS and sulfur Kβ XES. *a* shows the five selected compounds referenced to line colors used in *b* (lower plots) and in *c*–*e*. *b* shows example linear combination analyses of synthetic XAS and XES data with the fits (gray lines) and components shown below. Upper blue and red lines of *b* show synthetic XAS and XES respectively; these colors are chosen to be consistent with Figs. 3–5. Plots *c*–*e* show results of 40 different linear combination analyses for XAS, XES and combined XAS and XES, respectively. Ideal values fall on the diagonals. Vertical lines in *c*–*e* show estimated standard deviations obtained from the diagonals of the variance-covariance matrices. Component colors are shown in *a*.

TOC Figure